Effect of high pressure on competing exchange couplings in Li_2VOSiO_4

E. Pavarini,[1,2] S. C. Tarantino,[3] T. Boffa Ballaran,[4] M. Zema,[3,5] P. Ghigna,[6] and P. Carretta[1]
[1]*CNISM-Dipartimento di Fisica "A. Volta," Università di Pavia, I-27100 Pavia, Italy*
[2]*Institut für Festkörperforschung, Forschungzentrum Jülich, 52425 Jülich, Germany*
[3]*Dipartimento di Scienze della Terra, I-27100 Pavia, Italy*
[4]*Bayerisches Geoinstitut, Universität Bayreuth, 95440 Bayreuth, Germany*
[5]*CNR-IGG Sezione di Pavia, I-27100 Pavia, Italy*
[6]*Dipartimento di Chimica Fisica, Università di Pavia, I-27100 Pavia, Italy*
(Received 27 July 2007; revised manuscript received 24 October 2007; published 17 January 2008)

We report x-ray diffraction measurements on Li_2VOSiO_4 single crystals under pressures up to 7.6 GPa. The structure evolution under high pressure evidences a strongly anisotropic compressibility and a significant contraction of Li-O bonds. The corresponding evolution of the electronic structure was calculated *ab initio*. Using first-principles Wannier functions, we constructed, for several pressures, a (material-specific) low-energy one-band Hubbard model for the half-filled V *xy* bands. We found that the ratio between the next-nearest neighbor and nearest neighbor hopping integral, t_2/t_1, decreases by about 23% when the pressure increases from 0 to 7.6 GPa. By means of standard superexchange theory, we estimated a corresponding decrease of about 40% in the ratio J_2/J_1 between the next-nearest neighbor and nearest neighbor magnetic coupling. This suggests that one could possibly tune the ground state of this frustrated two-dimensional antiferromagnet from collinear to disordered by applying high pressures.

DOI: 10.1103/PhysRevB.77.014425 PACS number(s): 75.30.Et, 73.21.−b, 61.05.cp, 71.27.+a

Frustration of the exchange couplings is known to enhance the quantum fluctuations and to lead to the onset of novel disordered ground states.[1] Accordingly an intense research activity on frustrated magnets has emerged and prototype compounds have been synthesized. Particular attention has been addressed to the two-dimensional $S=1/2$ systems, frustrated either by the spin lattice geometry, as the Kagomé lattice compounds,[2] or by the geometry of the interactions, as the J_1-J_2 model on a square lattice.[3] The latter model has received much attention after the discovery of Li_2VOSiO_4, which is characterized by a square-lattice arrangement of $S=1/2$ V^{4+} ions, interacting either through nearest neighbor (J_1) or next-nearest neighbor (J_2) antiferromagnetic exchange couplings.[4] Li_2VOSiO_4 is characterized by $J_2/J_1>1$,[5–7] namely, it is deeply in the part of the phase diagram characterized by a collinear ground state.[3] Recently, other prototypes of the J_1-J_2 model have been synthesized, either with positive or negative values of J_2/J_1.[8] Despite the efforts in the chemical synthesis of novel materials none of the compounds grown so far lies in the most debated region of the phase diagram with $J_2/J_1>0$, the one with $J_2/J_1 \simeq 0.5$ where a disordered ground-state is expected.[3] In fact, although it seems well established that for $J_2/J_1=0.5$ long-range order should be suppressed, there is no general consensus on which should be the ground state in this region and up to which values of J_2/J_1 the disordered ground state should exist.

In order to tune the ratio between the exchange couplings one could think of adopting an approach which is alternative to the chemical one, as the application of a high pressure (P). In view of the possibility to apply P of several GPa by means of diamond anvil cells (DAC) one could envisage to modify the structure and tune the overlap among the atomic orbitals involved in the superexchange couplings with high P. Accordingly, in order to affect the J_2/J_1 ratio and possibly approach the 0.5 region, we have applied pressures up to 7.6 GPa on Li_2VOSiO_4 single crystals and investigated the structure modifications with x-ray diffraction (XRD) measurements. Then, using density functional theory in the local density approximation (LDA), we have calculated *ab initio* the corresponding variation in the hopping integrals of the partially filled V *xy* band. Finally, by using superexchange theory, we have estimated the pressure-induced modifications of the competing magnetic exchange couplings. This procedure has already been successfully used to estimate the exchange couplings of other prototypes of the J_1-J_2 model.[9] We find that upon increasing P J_2/J_1 decreases and possibly approaches the part of the J_1-J_2 phase diagram characterized by a disordered ground state.

Li_2VOSiO_4 structure (tetragonal, space group $P4/nmm$) is formed by piling up parallel $[VOSiO_4]_n^{2-}$ layers containing VO_5 square pyramids, enclosed in a Li tetragonal cage, sharing corners with SiO_4 tetrahedra[10] (see Fig. 1). Each pyramid is made of four equivalent basal oxygens (O1) and an apical oxygen (O2), and has a V at about the center (~1.6 Å below O2, and distant ~1.9 Å from the basal O1 atoms). In each layer two nearest neighbor VO_5 pyramids point alternatively downward (sites 1 in Fig. 1) or upward (sites 2 in Fig. 1). The V atoms in a layer form pseudosquare lattices with axes $(\mathbf{a}+\mathbf{b})/2$ and $(\mathbf{a}-\mathbf{b})/2$,with two near neighbor V atoms (the V at site 1 and the V at site 2 in Fig. 1) displaced along $\mathbf{c}$ by $z_V\mathbf{c}$ and $(1-z_V)\mathbf{c}$, respectively.

Single crystals of Li_2VOSiO_4 were prepared following the procedure reported in Ref. 11. XRD measurements were performed on two single crystals, LiV5b and LiV4b hereafter, with dimensions $0.22\times0.18\times0.07$ mm^3 and $0.18\times0.15\times0.12$ mm^3, respectively. The crystal quality was preliminarily checked by in air single-crystal diffraction analysis using the same procedure described in Ref. 11. Structure refinements converged to final agreement indexes

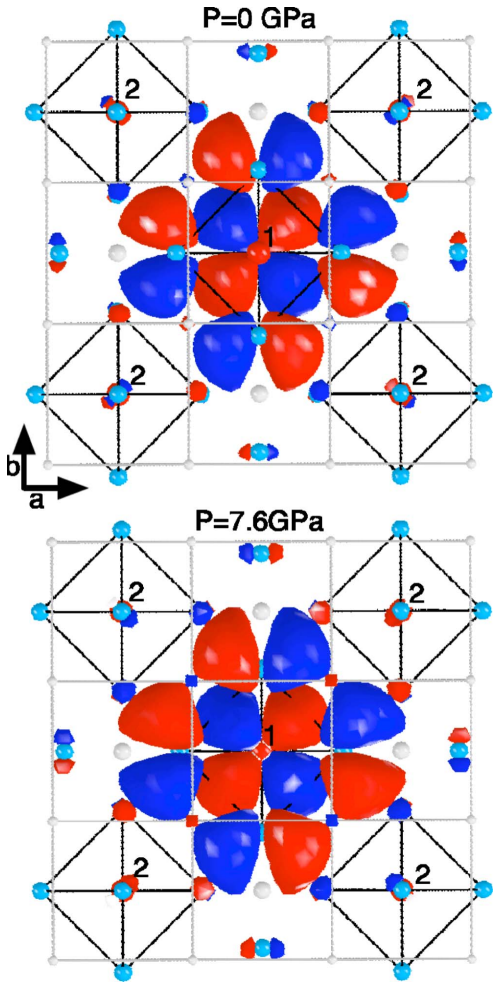

FIG. 1. (Color online) Structure (top: ambient P; bottom: $P=7.6$ GPa) of Li_2SiOVO_4, composed of VO_5 pyramids in a tetragonal Li cage with a Si close to the center. V is red; O blue; Si and Li (small) gray. A primitive cell contains two formula units, and thus two pyramids (the ridges are shown as black lines); the pyramid around the V in $(1/4,1/4,z_V)$ (site 1, at the center) points downward and that around the V in $(-1/4,-1/4,1-z_V)$ (site 2) upward. The xy Wannier function is superimposed to site 1; red (blue) is positive (negative). Increasing the pressure, the lattice contracts and the xy Wannier orbital becomes more extended in the xy plane.

$R_1=1.98\%$ for LiV5b (calculated on 303 independent reflections) and 2.19% for LiV4b (calculated on 302 independent reflections) with no significant electron density residuals. In order to perform XRD measurements under high P each crystal was loaded into a BGI (Bayerisches Geoinstitut) design DAC.[12] Steel gaskets preindented to thicknesses of 100–110 μm and with hole diameters of 300 μm were used. A 4:1 mixture of methanol:ethanol was used as a hydrostatic pressure-transmission medium. In order to have the ac plane on the diamond culet inside the DAC, crystal LiV4b was preliminarily oriented, embedded in epoxy resin, and cut to final crystal dimensions $0.11\times0.05\times0.03$ mm^3. This orientation was chosen as it allows us to collect the maximum number of reflections while the crystal is in the DAC. Pressure was determined from the unit-cell parameters on the basis of the equation of state for Li_2VOSiO_4, previously determined by Tarantino *et al.*,[13] so that the superposition of diffraction spots from ruby chips or quartz was avoided. At each pressure, lattice parameters were determined with a Huber single-crystal diffractometer with point-counter detector from a list of 17–22 reflections for crystal LiV5b and of 7–10 reflections for crystal LiV4b. Full details on the instrument and the peak-centering algorithm are provided in Ref. 14. Five complete XRD datasets at different P have then been collected on each crystal (in the range 0–6.12 GPa for LiV5b and 0–7.6 GPa for LiV4b) using an Oxford Xcalibur four-circle diffractometer. The diffracted intensities were corrected for absorption according to the semiempirical method of Blessing.[16] Reflections partially superimposed to diffraction spots from diamonds or Be rings were omitted before applying absorption correction.

Structure refinements were carried out in space group $P4/nmm$ by full-matrix least-square fits using SHELXL-97[17] and the atomic scattering curves from the International Tables of X-ray Crystallography.[18] In the present work structural data from the crystal LiV4b only have been used. The orientation of LiV5b crystal in the DAC allowed us to detect only reflections with $-1\leq l\leq 1$, yielding highly correlated z/c atomic fractional coordinates. The R factors, related to the difference between F_o and F_c (the measured and calculated structure factors, respectively), were fairly higher for LiV4b due to its reduced size which allowed to detect fewer reflections, nevertheless no unacceptable structural features have been observed. Data from LiV5b showed better internal agreement indexes owing to the higher peak intensity. The validity of the refined structural models for LiV4b was cross-checked by calculating the discrepancy factors R between F_c calculated from the refined atomic positions of LiV4b and F_o from XRD data collected on LiV5b at the same pressure. These values are fairly low and between 2.80 and 3.51%. The values of tetragonal symmetry-constrained unit cell parameters obtained by vector-least-squares fits[15] together with the details of XRD data collections and structure refinements on crystal LiV4b are reported in Table I. Final fractional atomic coordinates and isotropic displacement parameters U_{iso} are reported in Table II, whereas the interatomic distances and selected geometrical parameters are reported in Table III. After the end of the cycle of high P experiments, crystal LiV5b structure was checked again with XRD by collecting data up to $2\theta=118.8°$. Structure refinement converged to final R of 1.99% on 755 independent reflections. An excellent agreement with the structure determined before loading the sample in the DAC was found, showing that no hysteresis or crystal defects were caused by the high P cycles.

The compressibility of Li_2VOSiO_4 is strongly anisotropic with the a axis four times less compressible than the c axis.[13] As evident in Table III, the Li-O distances display the greatest compression and cause an octahedral volume decrease of about 8.8% upon increasing P up to 7.6 GPa. It is worth noting that the Li octahedron becomes significantly more distorted with increasing pressure being the longer Li-O2 apical bonds approximately 30% less compressible than the

TABLE I. The pressure dependence of the lattice parameters is reported with details on structure refinements on crystal LiV4b. Standard deviations are in parentheses. All structure refinements, carried out in space group $P4/nmm$, reached convergence (shift/e.s.d.=0.0000).

	RP	0.8(1) GPa	2.4(1) GPa	5.8(1) GPa	7.6(1) GPa
a (Å)	6.374(2)	6.366(3)	6.345(2)	6.314(2)	6.301(1)
c (Å)	4.454(6)	4.430(5)	4.391(3)	4.304(3)	4.262(3)
V (Å^3)	181.0(3)	179.5(2)	176.8(2)	171.6(1)	169.2(1)
D_{calc} (g×cm^{-3})	3.173	3.199	3.248	3.347	3.394
μ (mm^{-1})	2.96	2.98	3.03	3.12	3.16
Reflns measured	1032	945	974	864	922
Reflns unique	112	99	105	95	96
Reflns with $I>2\sigma_I$	102	91	95	85	88
R_{int}(%)	11.54	13.72	19.43	11.67	14.30
R_{sigma}	4.71	5.26	8.20	4.70	5.87
R_1[a](%)	6.81	7.36	7.24	7.06	7.01
R_{all} (%)	7.80	7.74	7.97	7.64	7.66
wR_2 (%)	16.04	15.92	17.89	17.84	14.59
GOF[b]	1.133	1.160	1.174	1.109	1.211
max, min $\Delta\rho(e$ Å$^{-3})$	1.90,–0.68	1.30,–0.68	2.05,–1.34	1.50,–0.83	0.86,–0.73

[a]$R_1=\Sigma||F_o|-|F_c||/\Sigma|F_o|$ (calculated on reflections with $I>2\sigma_I$).
[b]GOF=$S=[\Sigma[w(F_o^2-F_c^2)^2]/(n-p)]^{0.5}$, where n is the number of reflections and p is the total number of refined parameters. $\Delta\rho$ gives the minimum and maximum electron density residuals. RP is the ambient pressure.

Li-O1 square planar bonds. On the other hand, the contraction of the four V-O1 bonds by approximately 1.3% and of the V-O2 vanadyl bond by about 1.8% yields a polyhedral compression of about 4.2%. Tetrahedral Si-O bonds are even less compressible than the V-O ones. In fact, Si-O length decreases by about 1.2% between ambient pressure and 7.6 GPa, causing a reduction of the SiO_4 tetrahedral volume by about 3.4%. The evolution of the volume of the polyhedra with P was fitted linearly for simplicity, owing to the small number of data points. Single polyhedral bulk moduli were calculated as the reciprocals of the mean compressibility coefficients taken from the linear fits and turned out to be 204.08, 86.2, and 212.76 GPa for V, Li, and Si polyhedra, respectively. The anisotropic response of Li_2VOSiO_4 structure under high P is also evident in the thermal expansion.[11] It was noticed that pressure and temperature have the opposite effect on the structural parameters. This applies to changes in unit-cell parameters, as discussed by Tarantino *et al.*,[13] and in some polyhedral deformations, as evident in Fig. 2 where the observed HP evolution of Li-O and Si-O mean bond distances are compared to the high temperature data of Zema *et al.*[11] Compression and expansion are larger perpendicular to the *ab* plane and the most relevant modifications as a function of P and T depend basically on the most flexible structural unit, the Li polyhedron.

In order to analyze the effect of the structural modifications on J_2/J_1 and to verify to what extent the system can be considered two-dimensional, we have determined the nearest-neighbors and next-nearest-neighbors hopping integrals from band-structure calculations.

First we have obtained the LDA bands[20] for the different structures (ambient P, P=2.4, 5.8, and 7.6 GPa). As a method we have adopted the nth-order muffin-tin orbital method.[21] At ambient pressure our LDA band structure is

TABLE II. Atomic fractional coordinates and equivalent isotropic displacement parameters (Å^2) for Li_2VOSiO_4 at different pressures. Standard deviations are in parentheses. U_{iso} are multiplied by 10^4. RP is the ambient pressure.

Site	Li	V		Si	O1			O2	
Wyckoff	4*e*	2*c*		2*a*	8*i*			2*c*	
position	(0,0,1/2)	(1/4,1/4,*z*)		(3/4,1/4,0)	(1/4,*y*,*z*)			(1/4,1/4,*z*)	
	U_{iso}	*z*/*c*	U_{iso}	U_{iso}	*y*/*b*	*z*/*c*	U_{iso}	*z*/*c*	U_{iso}
RP	375(68)	0.0863(2)	88(9)	64(11)	0.5435(2)	0.2166(4)	109(14)	–0.2802(10)	166(29)
0.8 GPa	264(66)	0.0868(7)	70(10)	51(13)	0.5421(15)	0.2166(14)	128(17)	–0.2805(12)	153(35)
2.4 GPa	212(72)	0.0878(6)	41(10)	40(12)	0.5423(12)	0.2197(12)	79(16)	–0.2819(29)	144(33)
5.8 GPa	121(44)	0.0923(5)	81(11)	105(14)	0.5432(12)	0.2239(11)	139(15)	–0.2821(26)	148(28)
7.6 GPa	168(54)	0.0914(7)	69(9)	86(13)	0.5432(11)	0.2242(13)	115(16)	–0.2848(33)	195(36)

TABLE III. Structural parameters for Li_2VOSiO_4 at different pressures. Standard deviations are in parentheses. Octahedral angle variance (OAV) and octahedral quadratic elongation (OQE) were defined in Ref. 19. RP is the ambient pressure.

	RP	0.8 GPa	2.4 GPa	5.8 GPa	7.6 GPa
			VO_5 *square pyramid*		
V-O1×4(Å)	1.957(6)	1.946(10)	1.943(8)	1.936(7)	1.932(7)
V-2(Å)	1.632(5)	1.627(5)	1.623(13)	1.611(12)	1.603(14)
O1-V-O1 (°)	84.93(7)	85.0(1)	84.9(1)	85.1(1)	85.1(1)
O1-V-O1 (°)	145.41(3)	145.6(4)	145.3(3)	146.0(3)	145.9(3)
O1-V-O2 (°)	107.3(1)	107.2(2)	107.3(2)	107.0(2)	107.0(2)
Polyhedral volume (Å^3)	5.152	5.076	5.054	4.976	4.936
			SiO_4 tetrahedron		
Si-O1×4(Å)	1.635(4)	1.635(8)	1.633(7)	1.623(6)	1.616(6)
O1-Si-O1 (°)	110.4(2)	110.2(3)	110.4(2)	110.6(2)	110.5(3)
O1-Si-O1 (°)	107.5(4)	108.1(5)	107.6(4)	107.1(4)	107.5(5)
Polyhedral volume (Å^3)	2.240	2.241	2.232	2.191	2.163
TAV	2.23	1.11	2.20	3.27	2.36
TQE	1.006	1.0003	1.0006	1.0008	1.0006
			LiO_6 octahedron		
Li-O1×4(Å)	2.050(3)	2.045(4)	2.026(3)	1.994(3)	1.984(3)
Li-O2×2(Å)	2.457(2)	2.452(2)	2.439(5)	2.421(4)	2.409(5)
⟨Li-O⟩ (Å)	2.186	2.181	2.164	2.136	2.126
O1-Li-O1(°)	180	180	180	180	180
O1-Li-O1 (°)	80.2(3)	80.0(5)	80.7(4)	82.0(4)	82.3(4)
O1-Li-O1 (°)	99.8(3)	100.0(5)	99.3(4)	98.0(4)	97.7(4)
O1-Li-O2 (°)	80.1(1)	79.8(2)	79.4(3)	78.7(2)	78.2(3)
O1-Li-O2 (°)	99.9(1)	100.2(2)	100.6(3)	101.3(2)	101.8(3)
O1-Li-O2 (°)	180	180	180	180	180
Polyhedral volume (Å^3)	13.226	13.099	12.780	12.283	12.066
OAV	106.22	111.35	113.33	115.98	121.91
OQE	1.0430	1.0445	1.0458	1.0482	1.0499

close to earlier results.[7,22,23] The oxygen p bands are completely filled and divided by a gap of about 1.5 eV from the narrow (bandwidth $W\sim 0.4$ eV) half-filled xy bands, while the remaining d states are empty. Next we downfold all degrees of freedom but the xy and construct a basis of localized xy Wannier functions which span these bands.[21,24] The band-energy dispersions can be written as follows:

$$\varepsilon_{\pm}(\mathbf{k}) = 2t_2(\cos k_a + \cos k_b) \pm 4t_1 \cos\frac{k_a}{2}\cos\frac{k_b}{2} - 2t_z \cos k_c + 4t_{2z}(\cos k_a + \cos k_b)\cos k_c + \cdots, \quad (1)$$

where $t_1=t^{(1/2)(1/2)0}$, $t_2=t^{100}$, $t_z=t^{001}$, $t_{2z}=t^{101}$ and $t^{lmn}=|t_{ij}|$, where t_{ij} are the hopping integrals from site i to site j distant $l\mathbf{a}+m\mathbf{b}+n\mathbf{c}$. The values of t^{lmn} are reported in Table IV for the different structures and up to the fourth near neighbors. Both Table IV and the Wannier function in Fig. 1 show that the basic effect of pressure is to increase the extension of the xy Wannier function in the ab plane, with a more sizeable increase of t_1, the hopping between nearest neighbors.

The Hamiltonian which describes the low-energy properties of Li_2SiVO_4 is then a one-band Hubbard model $H=\Sigma_{ij\sigma}t_{ij}c^{\dagger}_{i\sigma}c_{j\sigma}+U\Sigma_i n_{i\uparrow}n_{i\downarrow}$ where $c^{\dagger}_{i\sigma}$ creates a xy electron with spin σ at site i, $n_{i\sigma}=c^{\dagger}_{i\sigma}c_{i\sigma}$, and U is the on-site screened

TABLE IV. Hopping integrals t^{lmn} (in meV) from site i to site j distant $l\mathbf{a}+m\mathbf{b}+n\mathbf{c}$ and for different pressures (in GPa). $P=0$ corresponds to ambient pressure. The hopping integrals are given up to the fourth nearest neighbors. Further hopping integrals are small and may be neglected. The magnetic couplings J_i (in K) are obtained by standard superexchange theory as $J_i\sim t_i^2/U$, using $U=5$ for the screened Coulomb interaction. Notice that the ratio J_2/J_1 is independent of U up to order t_i/U.

P/lmn	001	$\frac{1}{2}\frac{1}{2}0$	100	101	110			
	t_z	t_1	t_2	t_{2z}	t_4	J_1	J_2	J_2/J_1
0	13.3	10.0	37.0	4.9	5.3	0.9	12.7	13.7
2.4	13.8	11.2	38.4	5.1	5.9	1.2	13.7	11.9
5.8	14.6	14.0	42.2	5.4	6.5	1.8	16.5	9.1
7.6	14.6	15.0	42.5	5.4	6.7	2.1	16.8	8.0

Coulomb repulsion. A reasonable estimate of U in vanadium oxides is 4–5 eV.[22,27] Since the xy electrons are strongly localized around their own site and the VO_5 are not directly connected, the Coulomb repulsion between nearest neighbors or further sites can be neglected.[7,22]

Since t^{lmn}/U is small, we calculate the magnetic couplings by using standard superexchange theory.[26] In this approximation, the magnetic exchange couplings are given by $J^{lmn} \sim 4|t^{lmn}|^2/U$. Notice that, while $J_1 = J^{(1/2)(1/2)0}$ and $J_2 = J^{100}$ strongly depend on U, which is known only within an error of the order of the eV, the ratio J_2/J_1 is U-independent up to order t^{lmn}/U. Results for the ratio J_2/J_1 are displayed in Table IV. It is observed that the ratio significantly *decreases* (about 40%) upon increasing P up to 7.6 GPa.

From our calculations $J_2/J_1 \simeq 14$ at ambient P, which indicates that Li_2VOSiO_4 lies in the part of J_1-J_2 model phase diagram characterized by a collinear ground state. Although this ground state has been confirmed by several experiments, the analysis of susceptibility, specific heat, and NMR $1/T_1$ data rather suggests a value $1 \leq J_2/J_1 \leq 5$[5]; namely, that this vanadate is not far from the part of the phase diagram characterized by a disordered ground state. Still, these estimates depend on the theoretical model used to analyze the data. In fact, from high temperature expansions a ratio of J_2/J_1 larger than 10 can be estimated.[25] Here we want to stress that even if the precise value for this ratio is not known, the observation that J_2/J_1 is decreasing with pressure is rather promising, since it indicates that under high P Li_2VOSiO_4 could approach the part of the phase diagram characterized by a disordered ground state and which is subject of an intense scientific debate.

Finally, it is interesting to observe the effect of pressure on the exchange coupling along the c axes. From ambient P up to 7.6 GPa the xy bands exhibit a very small dispersion along Γ-Z,[23] in agreement with the $P=0$ results reported in Ref. 22. This happens because of cancellations in Eq. (1), so that the dispersion along Γ-Z is $\propto -2t_\perp \cos k_c$, with $t_\perp \sim t_z - 4t_{2z} + \cdots$, and therefore weak,[23] and sensitive to details. t_z and t_{2z} themselves are at $P=0$, 13, and 5 meV, respectively, and slightly larger at $P=7.6$ GPa. This evidences a nonnegligible coupling along the c axes, which can justify the long-range magnetic order observed by means of NMR measurements[4] and resonant x-ray scattering[6] at ambient P.

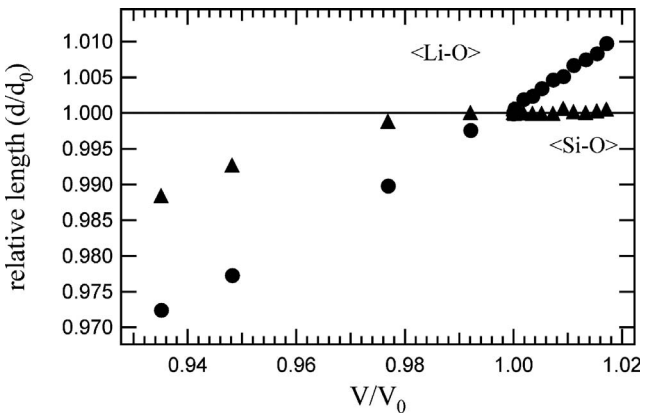

FIG. 2. Variation of relative average Si-O (triangles) and Li-O (circles) bond lengths as a function of V/V_0, where V_0 is the unit cell volume at ambient P and T. HT data from Ref. 11. Circles: Average Li-O bond distances; triangles: Si-O bond lengths. The figure shows that there are no significant differences between polyhedral expansion and compression.

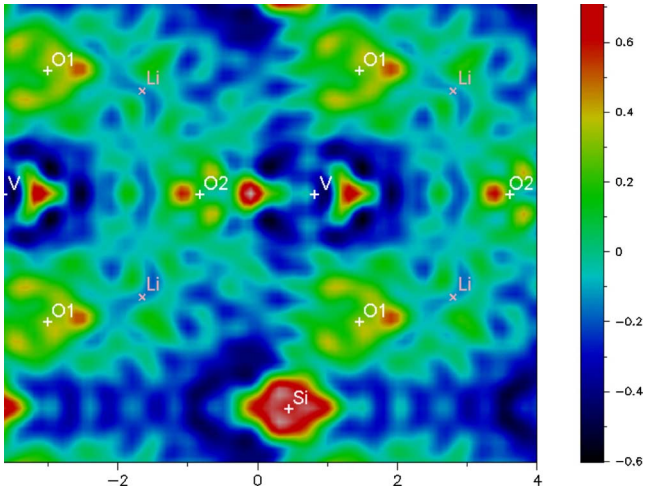

FIG. 3. (Color online) Electron density distribution for LiV5b in the ac plane at $y/b=0.25$ level, derived from the F_o-F_c map after the high P experiments. Relative distances in Å are reported on the axes. Li x,z coordinates are also indicated.

Still, the exchange couplings in Li_2VOSiO_4 are basically two-dimensional at ambient pressure. The absence of any significant orbital overlap along the c axes is also supported by the electron density distribution in the ac plane, which we derived from the Fourier transform of the XRD pattern (Fig. 3). One notices that the electron density in between V layers is extremely reduced. This suggests that at ambient P the strength of J_z and J_{2z} could be overestimated. Upon increasing P, the 3D magnetic couplings could, however, become more important. Nevertheless, we found that, up to 7.6 GPa, despite of the sizeable contraction of c axes, the effect on t_z and t_{2z} seems to be minor (Table IV). Both t_z and t_{2z} increase very weakly (less than 10%) with increasing the pressure up to 7.6 GPa, while t_1 increases rapidly (about 50%). Hence, if the structure is 2D at ambient pressure, also under higher P the spin lattice could remain basically two-dimensional and 3D long-range order could be confined in the very low temperatures regime.

In conclusion, from the analysis of the effect of the structural modifications on Li_2VOSiO_4 exchange couplings, based on band structure calculations, we show that upon increasing pressure J_2/J_1 decreases, possibly approaching the part of the phase diagram of the J_2-J_1 model characterized by a disordered ground state. Although the absolute values of the exchange couplings can suffer from the uncertainties implicit in the calculation method, the trend of J_2/J_1 should be considered as significant. We believe that these results will trigger novel studies of Li_2VOSiO_4 magnetic properties under high P.

This work has been partially supported by Italian MIUR (PRIN 2006) project "Experimental studies on geological materials at high pressure and temperature: implications for

the Earth system." High pressure diffraction experiments were performed at the Bayerisches Geoinstitut under the EU "Research Infrastructures: Transnational Access" Programme [Contract No. 505320 (RITA)–High pressure]. Calculations were done in Jülich under Project No. JIFF2200. We thank G. Bihlmayer for help with the FLEUR code.

[1] See H. T. Diep, in *Frustrated Spin Systems* (World Scientific, Singapore, 2004).
[2] P. Mendels, F. Bert, M. A. de Vries, A. Olariu, A. Harrison, F. Duc, J. C. Trombe, J. S. Lord, A. Amato, and C. Baines, Phys. Rev. Lett. **98**, 077204 (2007).
[3] P. Chandra, P. Coleman, and A. I. Larkin, Phys. Rev. Lett. **64**, 88 (1990); H. J. Schulz and T. A. L. Ziman, Europhys. Lett. **18**, 355 (1992); N. Shannon, T. Momoi, and P. Sindzingre, Phys. Rev. Lett. **96**, 027213 (2006); N. Shannon, B. Schmidt, K. Penc, and P. Thalmeier, Eur. Phys. J. B **38**, 599 (2004).
[4] R. Melzi, P. Carretta, A. Lascialfari, M. Mambrini, M. Troyer, P. Millet, and F. Mila, Phys. Rev. Lett. **85**, 1318 (2000).
[5] P. Carretta, N. Papinutto, R. Melzi, P. Millet, S. Gouthier, P. Mendels, and P. Wzietek, J. Phys.: Condens. Matter **16**, S849 (2004).
[6] A. Bombardi, J. Rodriguez-Carvajal, S. Di Matteo, F. de Bergevin, L. Paolasini, P. Carretta, P. Millet, and R. Caciuffo, Phys. Rev. Lett. **93**, 027202 (2004).
[7] H. Rosner, R. R. P. Singh, W. H. Zheng, J. Oitmaa, and W. E. Pickett, Phys. Rev. B **67**, 014416 (2003).
[8] N. S. Kini, E. E. Kaul, and C. Geibel, J. Phys.: Condens. Matter **18**, 1303 (2006).
[9] P. Carretta, N. Papinutto, C. B. Azzoni, M. C. Mozzati, E. Pavarini, S. Gonthier, and P. Millet, Phys. Rev. B **66**, 094420 (2002).
[10] P. Millet and C. Satto, Mater. Res. Bull. **33**, 1339 (1998).
[11] M. Zema, S. C. Tarantino, P. Ghigna, and G. Montagna, Z. Kristallogr. **222**, 350 (2007).
[12] D. R. Allan, R. Miletich, and R. J. Angel, Rev. Sci. Instrum. **67**, 840 (1996).
[13] S. C. Tarantino, M. Zema, T. Boffa Ballaran, and P. Ghigna (unpublished).
[14] R. J. Angel, in *High-Temperature and High-Pressure Crystal Chemistry. Reviews in Mineralogy and Geochemistry*, edited by R. M. Hazen and R. T. Downs (Mineralogical Society of America, Washington, DC, 2000), Vol. 41, p. 35.
[15] R. L. Ralph and L. W. Finger, J. Appl. Crystallogr. **15**, 537 (1982).
[16] R. H. Blessing, Acta Crystallogr., Sect. A: Found. Crystallogr. **51**, 33 (1995).
[17] G. M. Sheldrick, SHELX97—Programs for Crystal Structure Analysis (Release 97-2) (Institut für Anorganische Chemie der Universität, Göttingen, Germany, 1998).
[18] J. A. Ibers and W. C. Hamilton in *International Tables for X-ray Crystallography* (Kynoch Press, Birmingham, 1974), Vol. 4, pp. 99–101.
[19] K. Robinson, G. V. Gibbs, and P. H. Ribbe, Science **172**, 567 (1971).
[20] We used the scalar-relativistic approximation and the exchange-correlation potential of Perdew and Zunger. A different exchange-correlation potential may lead to differences of a few percents in the hopping integrals, but this systematic error does not affect the trends.
[21] O. K. Andersen and T. Saha-Dasgupta, Phys. Rev. B, **62**, R16219 (2000); Bull. Mater. Sci. **26**, 19 (2003).
[22] H. Rosner, R. P. Singh, W. H. Zheng, J. Oitmaa, S.-L. Drechsler, and W. E. Pickett, Phys. Rev. Lett. **88**, 186405 (2002).
[23] Our LDA calculations at $P=0$ yield a V xy bandwidth and hopping integrals slightly larger than those obtained in Refs. 7 and 22 with the LAPW method. However, this is a systematic error which does not affect the trends studied in the present paper (it is the same for all pressures). Furthermore, since in Refs. 7 and 22 the bands were plotted along Γ-X-M-Γ-Z only, in order to compare the strength of the k_z dispersion, we repeated the calculations using the LAPW FLEUR code (http://www.flapw.de) and calculated the bands also along A-M. We found that the k_c dispersion (i.e., t_z+4t_{2z}) is comparable with the one we obtained with the NMTO method. The special points here are $\Gamma=(0,0,0)$, $X=(\pi,0,0)$, $M=(\pi,\pi,0)$, $Z=(0,0,\pi)$, and $A=(\pi,\pi,\pi)$.
[24] E. Pavarini, A. Yamasaki, J. Nuss, and O. K. Andersen, New J. Phys. **7**, 188 (2005).
[25] E. E. Kaul, H. Rosner, N. Shannon, R. V. Shpanchenko, and C. Geibel, J. Magn. Magn. Mater. **272**, 922 (2004).
[26] We neglect the ferromagnetic contributions to the magnetic exchange couplings, which are expected to be very small because the V d electrons are localized and the VO_5 pyramids are not directly connected.
[27] T. Mizokawa and A. Fujimori, Phys. Rev. B **54**, 5368 (1996).